



Research Article

Analysis of self-consumption of energy from grid-connected photovoltaic system for various load scenarios with short-term buffering

Witold Marańda¹ 

© The Author(s) 2019 [OPEN](#)

Abstract

Energy from photovoltaics (PV) is becoming an important contributor to the energy mix for many countries. However, its impact on the distribution network is troublesome due the uncontrollable bidirectional transfers and might lead to the reduction in various forms of support for development of distributed PV systems in the future. This could be avoided by shifting from selling to self-consumption of PV energy, so the owner of PV would benefit mostly from reductions in energy purchase. This would also reduce overall power demand and transfer losses in the energy network, for the benefit of the climate. In order to achieve this goal, the PV system must be carefully adjusted to the local consumption profile and annual energy demand. The paper investigates the adjustment opportunities for the PV system with various local consumption scenarios and optional short-term energy buffering, with view of lowering the interaction with the utility grid. The simulation takes into account full-year period and gives guidelines for PV and battery sizing, presented for systems of any size.

Keywords PV system · Self-consumption · Energy storage · Energy balance

1 Introduction

The renewable energy systems (RES) together with distributed approach to energy generation are changing the existing power utility network for the benefit of their users and the climate.

The most widespread are the small, grid-connected photovoltaic systems, targeted to satisfy household or small enterprise energy demands. However, the integration of large numbers of small RES with distribution network creates technical problems such as excessive and uncontrollable transfers and energy quality issues [7]. Reaching the goal of 100% renewable grid, apart from technical issues, would require RES systems to be designed with main focus on matching supply and demand over multiple timescales [12].

The reduction in excessive grid traffic can be achieved by increasing the self-consumption of locally produced energy. This scenario corresponds with anticipated gradual withdrawal of various economic incentives fostering PV adoption in favor of low feed-in tariffs. Thus, the benefits from RES systems would change from selling energy to savings from lower purchases of grid energy.

Moreover, grid-traffic reduction can be combined with achieving the energy neutrality, when the system delivers as much energy as it consumes from the grid throughout the year. This might be of great importance for the utility grid if some long-term energy storage is to be implemented in the future.

The key to reach the goal of grid-traffic reduction and energy neutrality is the proper adjustment of PV generator to the local energy consumption, taking into account

✉ Witold Marańda, maranda@dmcs.pl | ¹Department of Microelectronics and Computer Science, Lodz University of Technology, Wolczanska 221/223, 90-924 Lodz, Poland.



climatic conditions and the use of short-term (day-to-night) energy buffering.

The existing research in the field of PV sizing is very broad, since there are many criteria, fields of applications, goals and climate specifics to be taken into account.

PV system and battery sizing versus load demand is of greatest importance for stand-alone PV systems, where the focus is on uninterrupted supply [11]. However, since there is no grid interaction, the sizing guidelines are not applicable for grid-connected systems.

For grid-connected systems, the research concerning self-consumption of energy concentrated on finding battery capacity versus PV array power, paying lower attention to the annual local energy consumption and its various types [15, 19].

Other works investigated the configuration of PV systems with local storage using country- or city-level consumption patterns [14] without addressing the issue of grid interaction. Others studied the system optimization for single particular loads according to economic metrics [1, 6], various feed-in tariffs [18] or demand balancing with PV arrays orientation [4].

Another important aspect of interaction of photovoltaics with the grid is the reduction in peak energy demands. The potential of PV systems with or without local storage for residential or office buildings was investigated [5, 10].

A new opportunity for PV-generated energy and successful RES integration is the growing popularity of electric vehicles. The research already shows the advantages of PV for electromobility [8, 13, 17], using car battery in various scenarios.

This work, in contrast, focuses on finding generic guidelines for increasing self-consumption and lowering grid traffic at the same time. The simulation model is stripped of unnecessary details, uses four generic energy consumption patterns and presents the results for the system of arbitrary size.

The input data for the guidelines are only two figures: anticipated annual PV energy yield and annual energy consumption: the data that are always easily available, regardless the complexity of the system.

2 System configuration and operation

The investigation focuses on a typical grid-connected PV system with a local load and an optional energy buffer. The configuration of both systems is shown in Fig. 1. The key components are: PV generator (P), local load (L), utility grid (G) and battery (B).

At any time, the electrical energy flows from some combination of sources (B , G , P) to some combination of sinks (B , G , L). Thus, the systems' operation can be

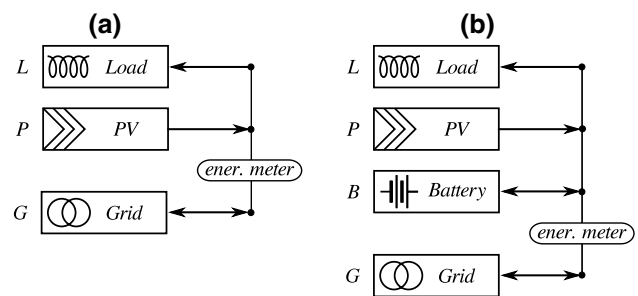


Fig. 1 System components and configuration

described in the form of a state diagram, as shown in Fig. 2, where the states represent energy flows.

The diagrams use the notation Source(s)→Sink(s) developed in [16], stating that in a particular moment any system component, despite its complexity, can be either energy sink or source and the changes are triggered by uncorrelated events in single components.

For the system without battery (Fig. 1a), grid (G) works as a backup supply for PV generator (P) and sinks the excess of PV energy. Therefore, only three states are possible here (Fig. 2a). At night, the load is supplied solely from the grid ($G→L$) and when solar energy becomes available, it contributes to load supply ($GP→L$). Finally, when solar power exceeds the load demand, its excess is fed to the grid ($P→GL$). Due to the varying nature of solar irradiance and load demand, the forward and backward transitions are very frequent throughout the day.

The load demand is always present (as defined in Sect. 4.2), and the instant PV startups or shutdowns are not considered.

The diagram for the system with battery (Fig. 1b) is more complex, since four components must follow additional rules:

- locally available energy always has the priority over grid,
- battery, when not empty, is capable to satisfy instant power demand,
- battery is charged only from excess of PV energy and never from grid,
- PV energy excess is fed to grid only when battery is full.

In contrast to Fig. 2a, the presence of the battery introduces an intermediate layer corresponding to autonomous operation; thus, grid and battery are never used together.

If solar power exceeds the load demand, the battery is charged ($P→BL$) and feeding to the grid is possible only when battery is full. If solar power cannot satisfy the load

Fig. 2 System operation diagrams: **a** without battery, **b** with battery

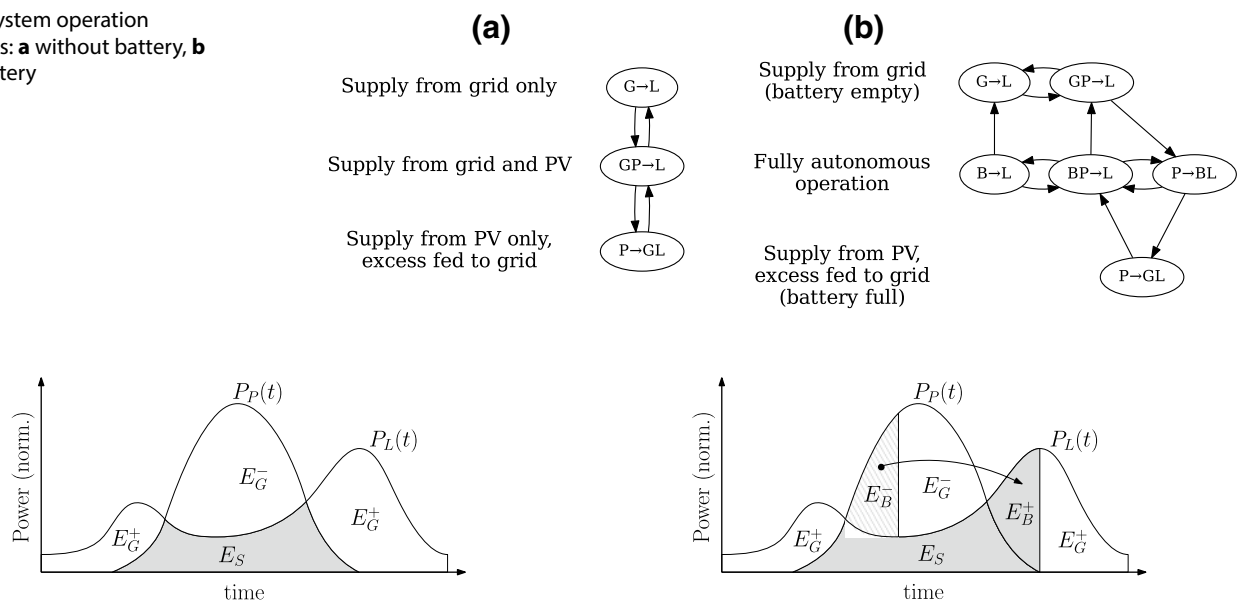


Fig. 3 Daily power profiles and energy shares (for system in Fig. 1a)

Fig. 4 Daily power profiles and energy shares (for system in Fig. 1b)

demand and battery is not empty, the load is still supplied from local sources only: $(BP \rightarrow L)$ or $(B \rightarrow L)$.

Fluctuations of irradiance and load demand trigger the transitions among all the states, and there are many paths within the diagram the system may take throughout the day.

3 Energy balance

The availability of solar energy and power demand from the load are the only driving factors for the system. Let $P_p(t)$, E_p and $P_L(t)$, E_L represent the instant power and energy shares of the PV generator and the load, respectively.

3.1 System without battery

According to Fig. 3, the energy consumed by the load (E_L) is delivered from PV generator (E_p) and utility grid (E_G^+). The excess of PV energy is fed to grid (E_G^-). The gray area (self-consumption E_S) represents the fraction of load demand which is satisfied solely from the locally produced energy.

Obviously, the shapes of $P_p(t)$ and $P_L(t)$ may be interwoven in more complex ways, but the separated areas (energy amounts) of the same meaning should be summed up.

The following relations can be identified from Fig. 3:

$$E_p = \int P_p(t)dt = E_G^- + E_S \tag{1}$$

$$E_L = \int P_L(t)dt = E_G^+ + E_S \tag{2}$$

Although Fig. 3 refers to a single day, Eqs. (1) and (2) will hold for any sequence of successive days. Since the analysis must span a representative period of time, let E_p , E_L , E_S , E_G^+ and E_G^- be the energy amounts for the full-year period.

From (1) and (2), it follows that difference in the amounts of local production and consumption is equal to the difference in grid energy transfers on a yearly basis:

$$E_p - E_L = E_G^- - E_G^+ = \Delta E_G \tag{3}$$

When the system is to be energy-neutral for a time period (i.e., produces as much as it consumes), the guiding rule for system sizing can be established:

$$\Delta E_G = 0 \iff E_p = E_L \tag{4}$$

It was demonstrated that energy-neutral system also generates minimal grid-traffic [17]. The rule (4) will be used as a reference point for other cases considered in the simulation, later in the paper.

3.2 System with battery

The purpose of battery is to increase the self-consumption by shifting the excess of PV energy to periods of its deficits, as shown in Fig 4. The E_B^- and E_B^+ represent energy accumulated and released from the battery, the gray area of E_S includes E_B^+ , and other symbols have the same meaning as in Fig. 3.

The energy balance equations take the form:

$$E_p = E_B^- + E_G^- + E_S - E_B^+ \tag{5}$$

$$E_L = E_G^+ + E_S. \tag{6}$$

The battery, in contrast to grid, can sink and source a finite amount of energy at a time, limited by its capacity C_B . For a single day, E_B^- may not be equal to E_B^+ , but that difference will never exceed C_B , no matter how many charge/discharge cycles the battery undergoes:

$$0 \leq |E_B^- - E_B^+| \leq C_B \tag{7}$$

When $C_B \ll E_L$, $E_B^- \approx E_B^+$ for a sufficient number of successive days and realistically sized system. This assumption is used in the simulation, and it reflects the fact that the battery storage has short-term character, rather than seasonal.

System with battery can reach energy neutrality under similar conditions. From (5), (6) and (7), it follows:

$$E_p - E_L = E_G^- - E_G^+ + E_B^+ - E_B^- \tag{8}$$

$$\Delta E_G = 0 \iff E_p = E_L \pm C_B. \tag{9}$$

With the realistic assumption of day-to-night buffering ($C_B \ll E_L$), the neutrality condition (9) becomes identical to (4).

It is worth noting that the presence of battery also reduces the grid traffic, since absolute values of E_G^- and E_G^+ in (8) are smaller than in (3).

3.3 Dimensionless parameters

The behavior of both systems from Fig. 1 can be fully derived from two key characteristics $P_p(t)$ and $P_L(t)$. The related values of E_p and E_L can be used as parameters for two-dimensional analysis of self-consumption energy E_S in terms of absolute values.

In order to make the results applicable to systems of arbitrary sizes and proportions, regardless the absolute energy values, the analysis was performed in function of just one dimensionless parameter:

$$E_{p/L} = \frac{E_p}{E_L}. \tag{10}$$

Then, the self-consumption of energy can be conveniently studied as dimensionless ratios in function of this parameter:

$$E_{S/L} = \frac{E_S}{E_L} = \eta_d(E_{p/L}) \tag{11}$$

$$E_{S/P} = \frac{E_S}{E_p} = \eta_u(E_{p/L}). \tag{12}$$

Those quantities can be interpreted as the “efficiency” of covering the load demand from locally produced PV energy (η_d) and “efficiency” to utilize PV energy locally (η_u). Both factors are closely related:

$$E_{S/P} = \frac{1}{E_{p/L}} E_{S/L}. \tag{13}$$

The change of $E_{p/L}$ makes both the factors to be inversely proportional, and they become equal for $E_{p/L} = 1$, which corresponds to the energy neutrality condition.

The introduction of energy buffer makes the battery capacity to be the second parameter for Eqs. (11) and (12); thus, the battery capacity also must be expressed as ratio to other energy quantities.

In contrast to annual values of E_p or E_L , the battery capacity should refer to daily transfers rather than annual, since it is designed for day-to-night charge/discharge cycles. For the period of analysis spanning n -days, let the battery capacity to be expressed as a dimensionless fraction of average daily energy demand (E_L/n):

$$C_{B/Ld} = n \frac{C_B}{E_L} \tag{14}$$

$$E_{S/L} = \frac{E_S}{E_L} = \eta_A(E_{p/L}, C_{B/Ld}) \tag{15}$$

$$E_{S/P} = \frac{E_S}{E_p} = \eta_E(E_{p/L}, C_{B/Ld}). \tag{16}$$

3.4 System examples

The results of analysis are given as values of $E_{S/L}$ and $E_{S/P}$. In order to interpret the results presented in Sect. 5, one must translate the absolute energy values into dimensionless parameters.

Table 1 gives some examples of systems having big differences in absolute values that are close to each other in terms of $E_{p/L}$, $C_{B/Ld}$ space. The parameters in the table are chosen with view to correspond to a few realistic PV systems, ranging from residential to small power plants.

The estimation of E_p from nominal PV power (in Table 1) is based on averaged energy yield for PV in Poland and the battery capacity is also expressed in terms of conventional 12 V lead–acid technology.

4 Simulation model

The simulation of systems from Fig. 1 requires PV power data $P_p(t)$ and consumption profiles $P_L(t)$ for the representative period of 1 year.

Table 1 Examples of systems and their parameters

	Nominal PV power (kWp)	E_p annual yield (kWh)	E_L annual cons. (kWh)	C_B bat. cap. (kWh)	C_B bat. cap. (Ah) at 12 V	$E_{p/L}$	$C_{B/Ld}$
1		1000	5000	0	0	0.2	0.0
3		3000	3000	4	342	1.0	0.5
50		50,000	20,000	11	913	2.5	0.2
500		500,000	1,000,000	274	22,831	0.5	0.1

The calculations were performed in terms of energy transfers in 5-s time steps. The operation of energy buffer is simplified: no charge/discharge losses or limits on current rates are considered.

The simulation software was custom-made in Python programming language, with the use of dedicated numerical and graphical libraries.

4.1 PV power profiles

Solar power generated by the PV generator E_p is computed according to standard approach as in [21] using solar irradiance as input data.

The irradiance (G) was recorded for the year 2018 in the Solar Lab of Lodz University of Technology with a calibrated CM21 Kipp & Zonen pyranometer, facing South at 30° inclination angle. The measurement was performed with the resolution of 5 s, and the collected data cover 97% of the period.

The ambient temperature (T_a) was also measured in order to calculate the temperature of PV cells (T_c), taking into consideration parameter $NOCT = 48\text{ }^\circ\text{C}$, as follows:

$$T_c = T_a + G(NOCT - 20)/800. \tag{17}$$

The temperature excess over 25° (standard test conditions) ΔT is then:

$$\Delta T = T_c - 25. \tag{18}$$

Since the power profile $P_p(t)$ must be normalized to give annual PV yield $E_p = 1$, the actual size of PV generator and conversion efficiency are both included in the normalization coefficient k . The computation of PV energy is done from global irradiance (at inclined plane) G_i , with correction for PV cells temperature:

$$E_p = k \sum_i G_i(1 + \beta\Delta T_i)\Delta t \tag{19}$$

where i goes through all the 5-s measurement intervals of Δt and the temperature coefficient β is assumed -0.5% —typical for silicon PV cells.

4.2 Load demand profiles

There exists a multitude of relevant electricity consumption profiles. Taking a household as an example, there are great differences in daily profiles due to heating/cooling needs [9], set of electrical appliances [2, 3] or habits of occupants [20], just to name a few reasons. Therefore, the some arbitrary selection was made in order to keep the conclusions more general and comparative.

The choice of energy consumption patterns was motivated to address a wide spectrum of real-life cases that share some similarities. Therefore, the proposed profiles emphasize the generic features of various daily energy consumption, i.e., a bimodal distribution for households, daily activity for offices, constant consumption for production plants or night charging of electric vehicles.

Four different types of load demand profiles $P_L(t)$ were prepared for the simulation. They are elaborated for the purpose of this article and do not borrow any data from other sources.

The profiles are prepared with 1-h time resolution for all days in a year, taking into account weekly and monthly variations. Separate daily profiles were prepared for weekdays, Saturdays and Sundays, and correction coefficient was applied for each month. All the $P_L(t)$ profiles are normalized over the year to fulfill the condition $E_L = 1$

For convenience, they are named as:

- *Household* (Fig. 5)—profile with two major power peaks and significant consumption decrease during summer months,

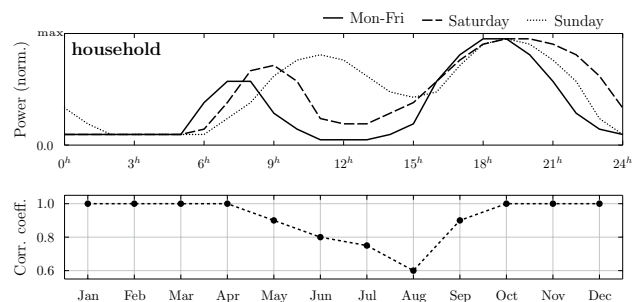


Fig. 5 Power demand profile of type “household”

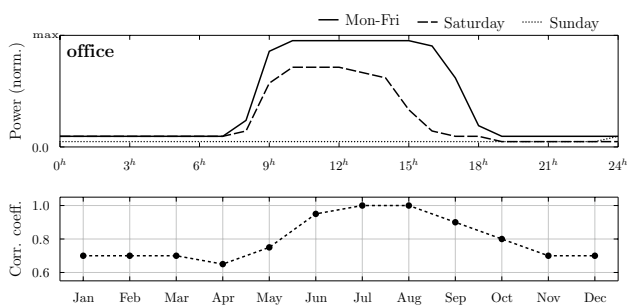


Fig. 6 Power demand profile of type “office”

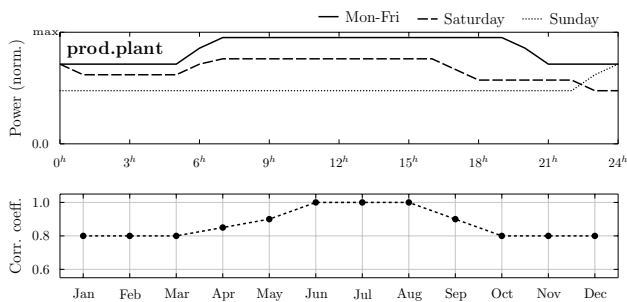


Fig. 7 Power demand profile of type “production plant”

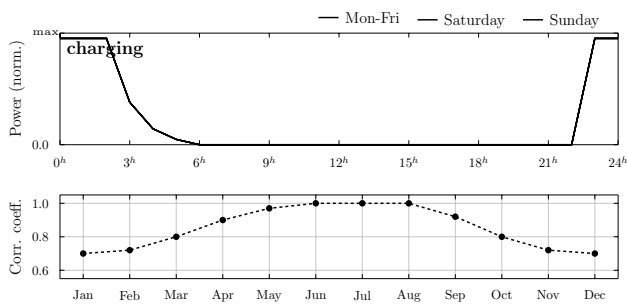
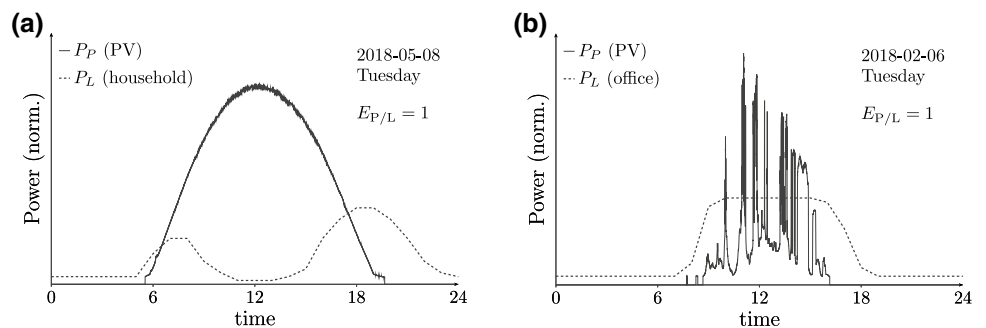


Fig. 8 Power demand profile of type “charging”

Fig. 9 Examples of normalized power profiles: household and office



- Office (Fig. 6)—profile with daytime peak, reduced activity on Saturdays, shutdown on Sundays and increased consumption in Summer,
- Production plant (Fig. 7)—profile with nearly constant consumption over 24 h, with slight decrease during weekends,
- Charging (Fig. 8)—profile corresponding to overnight charging of electric vehicle, regardless of weekday, but with increased demand during summer months.

The names of profiles loosely correspond to the activities they may represent in real life. Obviously, such profiles cannot fit all, but—in author’s opinion—choosing a single particular real-life example would not be better.

This approach makes the conclusions more general and applicable to any systems that exhibit some resemblance to the generic patterns.

4.3 Power profiles examples

In order to illustrate the proportions of normalized power profiles $P_p(t)$ and $P_L(t)$, four various examples are shown in Figs. 9 and 10. All examples show single-day profiles, but the normalization was done for full year.

The profiles proportions reflect the ratio $E_{P/L} = 1$, which always leads to overproduction of PV energy in summer, for climate of Central Europe.

Figure 9a demonstrates mismatch between PV and household-type demand in summer, whereas Fig. 9b shows good match for office-type profile, but also highly variable PV power, very common in this climate.

Figure 10c, d represents the consumption types with the greatest mismatch between the production and consumption, leading to great daytime overproduction of PV in case of production plant, and total separation in case of charging profile.

Fig. 10 Examples of normalized power profiles: production plant and charging

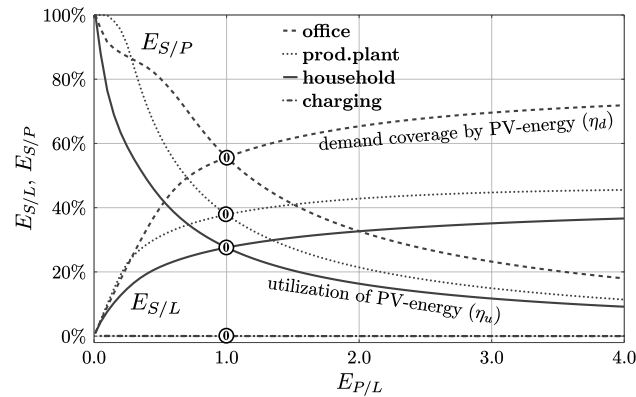
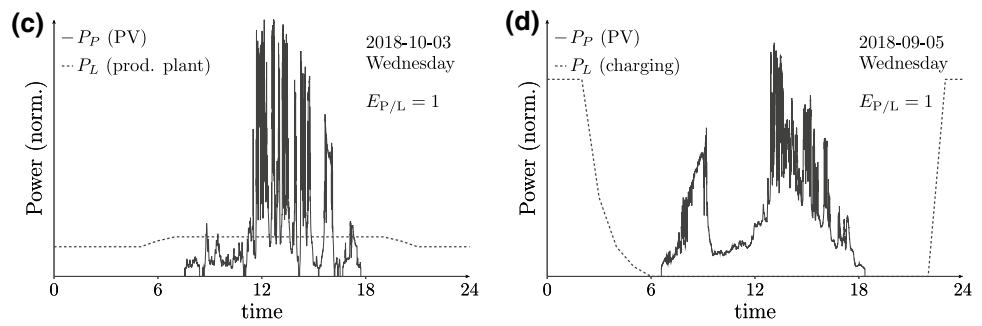


Fig. 11 $E_{S/L}$ and $E_{S/P}$ for all consumption profiles, without battery

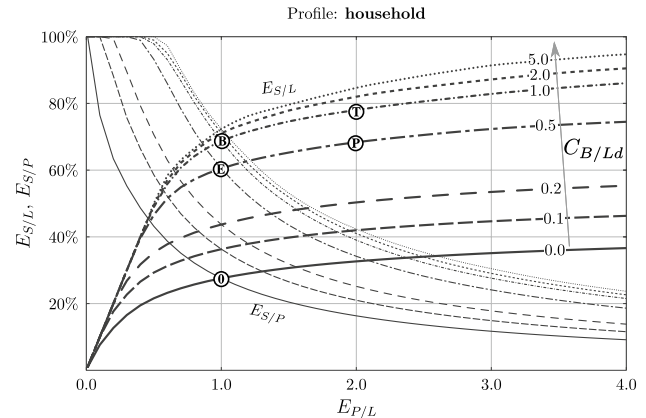


Fig. 12 $E_{S/L}$ and $E_{S/P}$ for household-type profile, with battery

5 Simulation results

The analysis of energy self-consumption was carried out as numerical computation of $E_{S/L}$ and $E_{S/P}$ in 2D space of $E_{P/L}$ and $C_{B/Ld}$ parameters.

According to (11) and (12), the factor $E_{S/L}$ has the interpretation of fraction of load demand that is covered from locally produced energy, whereas $E_{S/P}$ is a fraction of PV energy that can be utilized locally.

5.1 System with no energy buffer

The comparison of all four types of systems without battery is shown in Fig. 11. The horizontal axis gives the information how big is the PV generator versus load demand: 0.0 means no PV at all and 4.0 represents greatly oversized PV array. Since the values of $E_{S/L}$ / $E_{S/P}$ are energy proportions that can never exceed 1, the vertical axis displays percents.

The energy neutrality condition ($P_{P/L} = 1$) is marked with (0) symbol, where according to (4) always $E_{S/L} = E_{S/P}$. This point will serve as a reference for other results.

Household-type system, without energy buffering, can reach $E_{S/L}$ of only 30% at (0). Enlarging the PV

generator is not advisable in this case, since the improvement would be significant, at the cost of great increase in grid traffic.

For the office-type system, the value of $E_{S/L}$ can reach almost 60% at (0) due to the best match of its consumption to PV energy availability. In the extreme case, for the charging-type profile the results are always 0, since consumption and production do not overlap.

In all cases, however, increasing PV over $E_{P/L} = 1$ is not recommended. On the contrary, a smaller PV array sized down to $E_{P/L} = 0.5$ may be considered as cheaper and still delivering comparable $E_{S/L}$, but at a cost of higher energy purchase from the grid.

5.2 System with energy buffer

The presence of energy buffer in the system greatly improves both factors $E_{S/L}$ and $E_{S/P}$ for all types of consumption profiles. Figures 12, 13, 14 and 15 show the results for each profile type separately, for several values of battery capacity $C_{B/Ld}$, ranging from 0.0 to 5.0.

The interpretation of results is done for the following conditions:

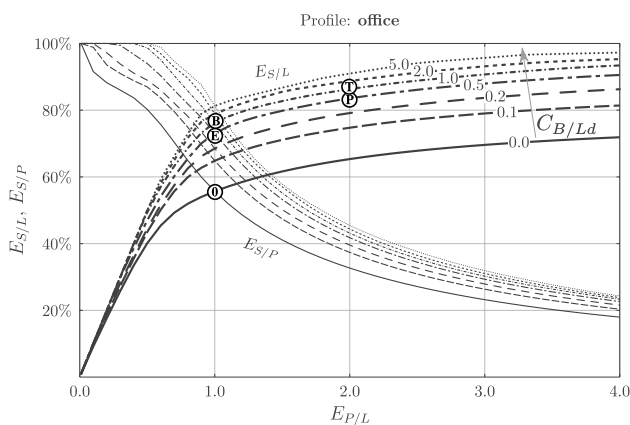


Fig. 13 $E_{S/L}$ and $E_{S/P}$ for office-type profile, with battery

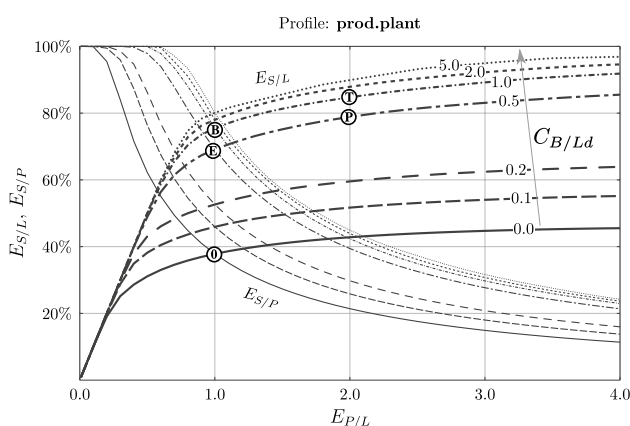


Fig. 14 $E_{S/L}$ and $E_{S/P}$ for production plant-type profile, with battery

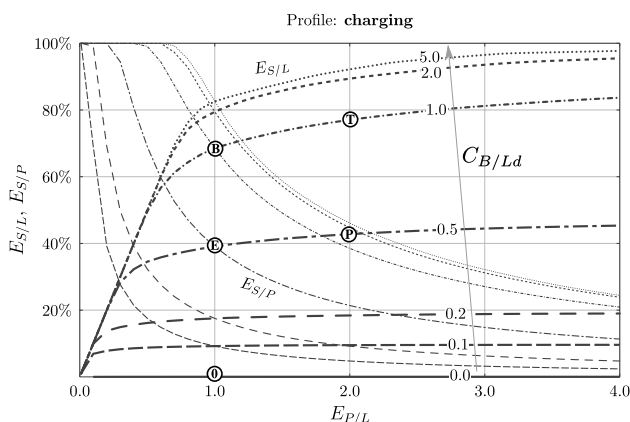


Fig. 15 $E_{S/L}$ and $E_{S/P}$ for charging-type profile, with battery

- (0)—(Zero) reference point for energy neutrality and lack of battery, any deviation from this condition involves higher grid traffic,
- (E)—(Economy) system with small battery of capacity $C_{B/Ld} = 0.5$ and the same PV array as for (0),

- (B)—(Battery) system with twice as big battery compared to (E), but with the same PV as for (0),
- (P)—(PV) system with twice as big PV array compared to (E), but with small battery as for (E),
- (T)—(Top) system with doubled both battery and PV size compared to (E).

For household-type system (Fig. 12), good results are achieved at (E), boosting $E_{S/L}$ from 30 to 60%. For better performance, any enlargement of PV must be done together with bigger battery (T), since points (B) and (P) alone offer no real improvement. Downsizing the PV below $E_{P/L} = 1$ is still a good alternative.

Both office and production plant-type systems (Figs. 13 and 14) achieve remarkable $E_{S/L} = 70\%$ at (E), and no further expansion is recommended. PV downsizing may be considered for production plant-type, but office-type with smaller PV would lose benefits of battery.

For charging-type system (Fig. 15), energy buffering changes everything dramatically. Here, a bigger battery is always better, up to capacity $C_{B/Ld} = 1.0$ at (B). At (E), $E_{S/L}$ reaches 40% and at (B) 70%. PV oversizing is not recommended, but downsizing is possible.

6 Conclusions

The paper analyzed the opportunities to increase the utilization of locally generated PV energy (i.e., the self-consumption-to-load demand ratio) with view to maintain equal balance between using and feeding energy to the grid and keeping the interaction with utility grid at minimal level.

The analysis was carried out by simulating the operation of PV system with various proportions of PV array and battery size versus own energy consumption and using day-to-night energy buffering.

The simulation was performed using the full-year (2018) solar data, for climate of Central Europe, and four various energy consumption patterns: “household,” “office,” “production plant” and “vehicle charging,” with weekly and seasonal variations.

The consumption cases represent the generic types of daily profiles, i.e., a bimodal distribution for households, daily activity for offices, constant consumption for production plants or night charging of electric vehicles.

In order to satisfy the energy neutrality condition and achieve the minimal grid traffic, it was found that the optimal size of PV array, in terms of annual yield, should match the annual demand of local energy consumption. The presence of battery does not change the energy neutrality, but further reduces the grid traffic

Under those conditions—without energy buffering—it is possible to reach 30–60% demand coverage from PV for “household,” “office” and “production plant” demand patterns. Optionally, PV array can be downsized to 0.5 of the optimal value and still maintain 20–50% of demand coverage annually. On the other hand, the PV oversizing is not recommended, since doubling the PV array size gives only few percent improvement, at the cost of increased grid traffic.

For “vehicle charging” profile, this coverage is zero due to the total mismatch in energy production and consumption.

The presence of relatively small battery can boost the demand coverage to 60–70%, lowering grid traffic at the same time. The recommended battery capacity, for “household,” “office” and “production plant” profiles, should be close to half of the average daily consumption. Increasing battery or PV size is not recommended, while PV downsizing may be considered.

Greatest benefits are observed for “vehicle charging” profile, where the demand coverage grows nearly proportionally to battery size, up to a recommended battery size, which is equal to average daily consumption.

The presented results have the merit of translating solar irradiance data and energy consumption patterns into simple guidelines for PV system sizing with energy neutrality and grid interaction in view. The input data for the guidelines are only: anticipated annual PV energy yield, annual energy consumption and resemblance to one of the generic energy consumption profiles.

The results are applicable to systems operating in climate of Central Europe, but the approach and the method are universal for systems of any size.

Compliance with ethical standards

Conflict of interest On behalf of all the authors, the corresponding author states that there is no conflict of interest.

Open Access This article is distributed under the terms of the Creative Commons Attribution 4.0 International License (<http://creativecommons.org/licenses/by/4.0/>), which permits unrestricted use, distribution, and reproduction in any medium, provided you give appropriate credit to the original author(s) and the source, provide a link to the Creative Commons license, and indicate if changes were made.

References

1. Angenendt G, Zurmühlen S, Axelsen H, Sauer DU (2018) Comparison of different operation strategies for pv battery home storage systems including forecast-based operation strategies. *Appl Energy* 229:884–899
2. Arghira N, Hawarah L, Ploix S, Jacomino M (2012) Prediction of appliances energy use in smart homes. *Energy* 48(1):128–134
3. Cetin K, Tabares-Velasco P, Novoselac A (2014) Appliance daily energy use in new residential buildings: use profiles and variation in time-of-use. *Energy Build* 84:716–726
4. Chattopadhyay K, Kies A, Lorenz E, von Bremen L, Heinemann D (2017) The impact of different pv module configurations on storage and additional balancing needs for a fully renewable european power system. *Renew Energy* 113:176–189
5. de e Silva GO, Hendrick P (2016) Lead-acid batteries coupled with photovoltaics for increased electricity self-sufficiency in households. *Appl Energy* 178:856–867
6. de e Silva GO, Hendrick P (2017) Photovoltaic self-sufficiency of belgian households using lithium-ion batteries, and its impact on the grid. *Appl Energy* 195:786–799
7. Elnozahy MS, Salama MMA (2013) Technical impacts of grid-connected photovoltaic systems on electrical networks: a review. *J Renew Sustain Energy* 5(3). www.scopus.com, cited By :36. Accessed Jan 2017
8. Elnozahy MS, Salama MMA (2014) Studying the feasibility of charging plug-in hybrid electric vehicles using photovoltaic electricity in residential distribution systems. *Electr Power Syst Res* 110:133–143. www.scopus.com, cited By :28. Accessed Jan 2018
9. Gouveia JP, Seixas J, Mestre A (2017) Daily electricity consumption profiles from smart meters-proxies of behavior for space heating and cooling. *Energy* 141:108–122
10. Jurasz J, Campana PE (2019) The potential of photovoltaic systems to reduce energy costs for office buildings in time-dependent and peak-load-dependent tariffs. *Sustain Cities Soc* 44:871–879
11. Khatib T, Ibrahim IA, Mohamed A (2016) A review on sizing methodologies of photovoltaic array and storage battery in a standalone photovoltaic system. *Energy Convers Manag* 120:430–448. www.scopus.com, cited By :39. Accessed Feb 2019
12. Kroposki B, Johnson B, Zhang Y, Gevorgian V, Denholm P, Hodge B, Hannegan B (2017) Achieving a 100 systems with extremely high levels of variable renewable energy. *IEEE Power Energy Mag* 15(2):61–73
13. Li X, Lopes LAC, Williamson SS (2009) On the suitability of plug-in hybrid electric vehicle (PHEV) charging infrastructures based on wind and solar energy. In: 2009 IEEE power and energy society general meeting, PES '09. www.scopus.com, cited By :70. Accessed Jan 2018
14. Lund PD (2018) Capacity matching of storage to PV in a global frame with different loads profiles. *J Energy Storage* 18:218–228. www.scopus.com, cited By :1. Accessed Dec 2018
15. Luthander R, Widén J, Nilsson D, Palm J (2015) Photovoltaic self-consumption in buildings: a review. *Appl. Energy* 142:80–94
16. Marańda W (2017) Diagrams for energy management in renewable energy systems. In: 2017 MIXDES—24th international conference mixed design of integrated circuits and systems, pp 475–478. <https://doi.org/10.23919/MIXDES.2017.8005257>
17. Marańda W (2018) Using solar energy for charging electric vehicles in Poland a case study. In: E3S web of conferences, vol 44. www.scopus.com. Accessed Nov 2018
18. Marańda W, Piotrowicz M (2014) Sizing of photovoltaic array for low feed-in tariffs. In: Proceedings of the 21st international conference on mixed design of integrated circuits and systems, MIXDES 2014, pp 405–408. www.scopus.com, cited By :4. Accessed Nov 2018
19. Martín-Chivelet N, Montero-Gómez D (2017) Optimizing photovoltaic self-consumption in office buildings. *Energy Build* 150:71–80
20. Tbal AM, Rajamani HS, Abd-Alhameed RA, Jalboub MK (2011) Identifying the nature of domestic load profile from a single

- household electricity consumption measurements. In: Eighth international multi-conference on systems, signals devices, pp 1–4. <https://doi.org/10.1109/SSD.2011.5993570>
21. Villalva MG, Gazoli JR, Filho ER (2009) Comprehensive approach to modeling and simulation of photovoltaic arrays. *IEEE Trans Power Electron* 24(5):1198–1208. www.scopus.com, cited By :2093. Accessed 2013

Publisher's Note Springer Nature remains neutral with regard to jurisdictional claims in published maps and institutional affiliations.